Chain Dynamics and Viscoelastic Properties of Poly(ethylene oxide)

K. Niedzwiedz,[†] A. Wischnewski,[†] W. Pyckhout-Hintzen,*[,†] J. Allgaier,[†] D. Richter,[†] and A. Faraone[‡,§]

Institute für Festkörperforschung, Forschungszentrum Jülich, 52428 Jülich, Germany, Department of Material Science and Engineering, University of Maryland, College Park, Maryland 20742, and NIST Center for Neutron Research, National Institute of Standards and Technology, Gaithersburg, Maryland 20899-8562

Received February 28, 2008; Revised Manuscript Received April 23, 2008

ABSTRACT: The chain dynamics and viscoelastic properties of poly(ethylene oxide) (PEO) were studied covering a wide range of molecular weights and temperatures. Two experimental techniques were used: rheology, in order to study the large scale viscoelastic properties, and neutron spin−echo (NSE) spectroscopy, to investigate the chain dynamics at the molecular level. We aimed to explore the characteristic dynamical parameters of the pure homopolymer system and describe its dependence on the polymer molecular weight and temperature. We will show that, after accounting for the molecular weigth dependence of the glass transition temperature, the dynamics observed for the different molecular weight samples can be consistently described by the Vogel−Tammann−Fulcher (VTF) temperature dependence.

I. Introduction

Poly(ethylene oxide) has a very wide field of applications. Its physicochemical properties are desired not only in industrial sectors but they are also very attractive for basic academic research. Due to its low cost and easy production PEO is often used for commercial purposes. For example, it can be used as a binder, in order to improve lubricity leading to easier mold release or as a flocculant for clay, effectively promoting its sedimentation.[1] It can be also effectively applied in the fluids transport through pipes where it functions to reduce the frictional resistance. Moreover, because of its safety (PEO being nontoxic and nonionic) it can be used in cosmetic products, where it is used as a thicker.[2] Recently, PEO started even to be employed in pharmaceutics as a base for orally administered controlled-release preparations.[3,4] Finally, PEO can be also used as an additive for polymerization reaction inhibiting foaming and promoting stable polymerization e.g. in production of vinyl chloride and acrylonitrile butadiene styrene.

From the perspective of academics research, one of the most prominent areas where PEO is used are rubbery electrolytes.[5,6] It is known that transport of salt ions is generally determined by ion−polymer interactions as well as local relaxation of the polymer; however, the understanding of this phenomenon on the molecular level is still poor. Another important field of interest is that of polymer blends, since PEO is miscible with many other polymer species.

The most prominent example is the PEO/PMMA blend, where the wide separation in the glass transition temperature of the pure components leads to a dynamical heterogeneity although it is perfectly miscible.[7] Finally, nanocomposites and fillers should be mentioned.[8] Here, the advantage of PEO is that it shows favorable interactions with the silicate surface, i.e., structural formations like the exfoliated, intercalated, or tactoidal states can be achieved without a priori modification of the silicate surface.

In spite of the variety of applications of PEO, both in industry and academic research, its characteristic dynamical parameters are still not well-known and have not been explored. Its high crystallization temperature $T_C \simeq 338$ K makes the system inapplicable for many experimental techniques.

We present a comprehensive and consistent study on the segmental dynamics and the viscoelastic properties of PEO. A series of studies on PEO with different molecular weights, between $M_w \simeq 1$ kg/mol, where the very short chains do not crystallize and are free of entanglements, up to highly entangled polymer chains ($M_w \simeq 932$ kg/mol), were performed. The measurements were done at various temperatures, depending on the experimental technique. We derived a consistent description of the dynamical properties of the PEO homopolymer system and its dependence on the molecular weight and temperature.

In the following, first the sample preparation and characterization, as well as the applied experimental techniques will be introduced (section II). In section III experimental results and their analysis are presented. Section IV addresses the discussion of the results. The basic concepts, Rouse dynamic for the short chain system and the reptation model for the long chain system, apply in the limiting cases for both techniques (neutron scattering and rheology); however, the extracted model parameters show a systematic discrepancy. Finally, in section V, the experimental outcome is summarized.

II. Experimental Section

A. Sample Preparation and Characterization. PEO samples were synthesized by living ring opening anionic polymerization at FZJ Jülich or obtained commercially from PSS Mainz and Scientific Polymer Products.[9] Polymerization was performed in tetrahydrofuran (THF) at $T = 323$ K using potassium as the counterion. The monomers of protonated and deuterated ethylene oxide (h_4 EO, d_4 EO) were purchased from CDN-isotopes (Quebeque, Canada, with 99.8% d). The monomers were purified twice with CaH_2. As initiators for EO-h_4 and EO-d_4, respectively, potassium *tert*-butoxylate and potassium *n*-hexoxylate were used. The samples were kept under high vacuum condition at 323 K in purified THF until the monomers were totally consumed. To terminate the process acetic acid was used. The polymers were precipitated in cyclohexane and dried under high vacuum. All samples were stored in closed vials in which air was replaced by argon gas as to avoid water takeup.

The characterization in terms of molecular weights and polydispersities (PD) was performed by size exclusion chromatography

* Corresponding author.
[†] Institute für Festkörperforschung, Forschungszentrum Jülich.
[‡] Department of Material Science and Engineering, University of Maryland.
[§] NIST Center for Neutron Research, National Institute of Standards and Technology.

10.1021/ma800446n CCC: $40.75
Published on Web 06/04/2008

Table 1. Molecular Characteristics of PEO Polymers

polymer	M_w [kg/mol]	M_w/M_n	T_m [K]
h-PEO[a]	0.89	1.04	306
h-PEO	2.12[b]	1.05	321
d-PEO	2.34[b]	1.05	321
h-PEO	81	1.13	338
d-PEO	108	1.19	338
h-PEO[c]	610	[d]	338
h-PEO[e]	932	[d]	338

[a] Sample purchased from Sigma-Aldrich Chemie GmbH (Steinheim, Germany). [b] M_w measured by NMR. [c] Sample purchased from Scientific Polymer Products, Inc. (Ontario, Canada). [d] Polydispersity not well defined for broad distributions, see text. [e] Sample purchased from PSS Polymer Standards Service (Mainz, Germany).

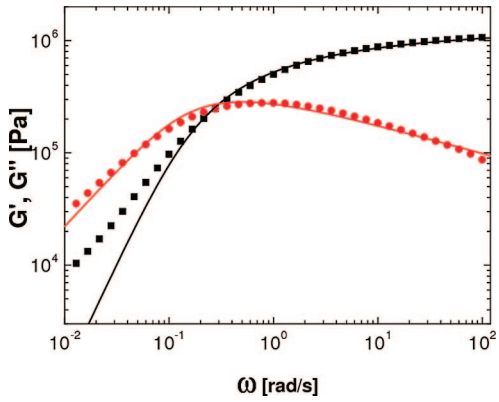

Figure 1. Rheology data for the PEO sample with $M_w = 932$ kg/mol measured at temperature $T = 378$ K. Black squares belong to the storage modulus, red circles to the loss modulus. Lines show fitting results obtained with the Winter ansatz. Deviations from the limiting slopes at low ω are due to polydispersity.

(SEC, PL-GPC 220) relative to narrow PEO standards using a 85/15 mixture of tetrahydrofurane and dimethylacetamide at 300 K as eluent. The molecular weights of the commercial high M_w samples were clearly not uniformly distributed and had polydispersities of 2 or higher. The companies did not provide an actual molecular weight distribution but only indicated small values ≈1.2 for the polydispersity. However, these monodisperse values were not reconfirmed by our own SEC measurements.

The glass transition temperature of the low molecular weight samples was estimated from the melting temperature. It was assumed that the ratio T_m/T_g[10] is constant for a given polymer species. For the high molecular weight sample, $T_g = 208$ K.[11]

The characteristic parameters of all used PEO samples as well as their origin are given in Table 1.

B. Rheological Measurements. The macroscopic rheological properties of PEO were studied on a strain-controlled ARES (Rheometric Sci /TA) instrument equipped with a 2 k FRTN1 force transducer. The main difficulty with mechanical spectroscopy for PEO samples is its crystallization at $T_C \simeq 338$ K. [The given value is for high molecular weight PEO $M_w \gtrsim 5$ kg/mol. With decreasing molecular weight, T_C decreases; for $M_w \simeq 1$ kg/mol, no crystallization is observed.] Therefore the accessible frequency window and the application of the time−temperature superposition are strongly restricted. The dynamic response of the short chain PEO system, probed by rheology, comprises 4 decades in frequency; i.e., it only covers the terminal flow regime and, only in case of high molecular weight and well entangled polymers, the characteristic loss peak in $G''(\omega)$ for reptation can be accessed. The faster Rouse-like processes remain far out of the probed frequency range and are localized at much higher frequencies which are prohibited by the onset of crystallization.

The low molecular weight sample ($M_w = 0.89$ kg/mol) was measured in a cone-plate geometry, with diameter $\phi = 25$ mm and a cone angle of 0.04 rad, keeping the gap spacing 0.051 mm. The sample was measured at four temperatures between 308 K ≤ T ≤ 323 K with a temperature step of $\Delta T = 5$ K. All independent isothermal frequency scans were performed using frequencies between 0.01 and 100 rad/s, with some cutoff at the low frequencies due to the limited resolution of the transducer.

Table 2. Viscosity of the PEO Sample with $M_w = 0.89$ kg/mol Obtained at Different Temperatures

T [K]	η_0 [Pa s]
308	0.126
313	0.110
318	0.087
323	0.071

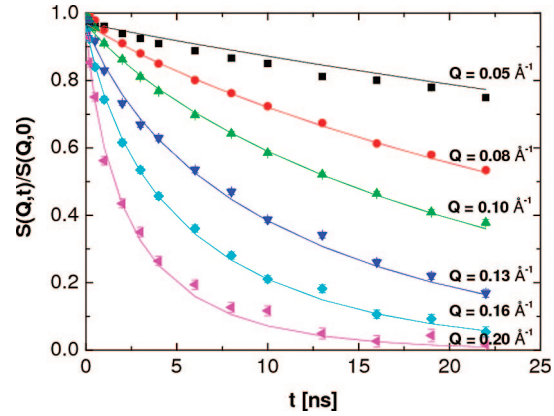

Figure 2. NSE data of a PEO sample with $M_w = 2.1$ kg/mol at $T = 413$ K. Symbols show the data measured for various Q values. Solid lines represent a fit with the Rouse model simultaneously to all Q's.

The measurements of the high molecular weight samples ($M_w = 610$ kg/mol and $M_w = 932$ kg/mol) were performed in the parallel plate geometry. Depending on the quantity of the available material, the samples were measured using plates of $\phi = 8$ mm with the gap spacing between 0.5 and 1 mm ($M_w = 610$ kg/mol) and $\phi = 25$ mm with the gap between 1 and 1.5 mm ($M_w = 932$ kg/mol). The samples were prepared into the required shape using a vacuum mold /press (10^{-3} mbar, $T \approx 373$ K). Measurements were done in the temperature range between 348 K ≤ T ≤ 468 K using a temperature-frequency sweep mode with $\Delta T = 15$ K. The isothermal frequency scans were performed in a frequency range between 0.01 and 100 rad/s. Applying the time−temperature superposition principle, the data were shifted to the requested reference temperature $T_0 = 348$ K and the shift factor a_T was obtained as

$$\log(a_T) = \frac{-C_1(T - T_0)}{C_2 + (T - T_0)} \quad (1)$$

following the well-known Williams−Landel−Ferry (WLF) equation. Furthermore, to check the precision of the time−temperature shifting and consistency, the sample with $M_w = 932$ kg/mol was successfully remeasured at the temperature $T = 378$ K over four decades in frequency range 0.01 ≤ ω ≤ 100 rad/s. In all the measurements the strain amplitude was kept small (5% for the low molecular weight sample and 1% for the high molecular weight samples) ensuring linearity of the response. A N_2 blanket prevents oxidation during the experiment. From SEC measurements after rheology for the narrow and polydisperse samples to check the molecular weight distribution degradation could be excluded.

C. Neutron Scattering. The chain dynamics was measured by neutron spin−echo spectroscopy (NSE).[12,13] To observe the single chain dynamic structure factor systems containing some protonated chains dissolved in the deuterated matrix were used. Here, the scattering rises from the contrast in the scattering length of the protons and deuterium; i.e., the main contribution to the scattering signal comes from the coherent scattering of the individual chain. To achieve reasonable scattering intensity the measured PEO sample contained 10% of h-PEO chains and 90% of d-PEO. Using polarized neutrons, the coherent scattering can be measured directly in terms

of normalized scattering function $S(Q, t)/S(Q, 0)$, where Q is the momentum transfer which depends on the neutron wavelenght λ and the scattering angle θ ($Q = (4\pi/\lambda)\sin(\theta/2)$). The scattering function relates to both the momentum and energy transfer; thus, it delivers information about both dynamics and structure.

The experiment on the low molecular weight sample ($M_w = 2.1$ kg/mol) was performed on the NSE spectrometer at the Research Centre Jülich (NSE-FZJ). The single chain dynamic structure factor was measured in a Q range from 0.05 to 0.20 Å $^{-1}$ at a temperature $T = 413$ K up to Fourier times of 22 ns using neutrons of $\lambda = 8$ Å.

In order to probe the dynamics of high molecular weight PEO ($M_w = 81$ kg/mol) the maximal Fourier time was extended to longer times. The investigation of the chain dynamic structure factor of the long chain polymer melt was performed at the NSE at National Institute of Standards and Technology (NIST), where for neutrons of $\lambda = 11.1$ Å the maximal Fourier time was 100 ns. The measurements were done at temperatures from 360 up to 450 K in a Q range between 0.05 and 0.20 Å^{-1}.

III. Results

A. Rheology. The experimental results for the commercial PEO with $M_w = 932$ kg/mol are presented in Figure 1.

The modulus data for high molecular weight samples were fitted to an empirical expression according to the phenomenological ansatz of Winter:[14]

$$\begin{aligned} H(\tau) &= H_e\tau^{n_e} + H_g\tau^{-n_g} \quad \tau_0 < \tau < \tau_{max} \\ H(\tau) &= 0 \qquad\qquad\qquad\quad \tau < \tau_0, \tau > \tau_{max} \end{aligned} \tag{2}$$

and

$$G(t) = \int_0^\infty \frac{H(\tau)}{\tau} \exp(-t/\tau)\, d\tau \tag{3}$$

and its dynamic analog $G^*(\omega)$ from Fourier transformation. τ_0 and τ_{max} are the shortest and longest relaxation times of the time distribution $H(\tau)$. H_e represents the entanglement regime and H_g the so-called glassy transition zone. The H_e and H_g are defined as:

$$H_e = n_e G_N^0 \tau_{max}^{-n_e} \tag{4}$$

$$H_g = n_g G_N^0 \tau_0^{n_g} \tag{5}$$

where n_e and n_g denote the slopes in the entanglement regime and the glassy transition zone, respectively. G_N^0 is the plateau modulus. Since the observed relaxation spectrum is restricted to the entanglement regime it was assumed that $H_g = 0$. The model gives a relatively good description of the data with a resulting plateau modulus $G_N^0 = 1.279$ MPa. The slope of $G''(\omega)$ at high $\omega \to \infty$ yields $n_e = 1/4$ as expected for well entangled polymers with negligible contributions from high ω Rouse modes. Deviations from the fit in the low frequency range are clear indications for polydispersity of the sample as well as the presence of bigger chain structures which are not accounted for in the polydispersity index (see in Figure 1) but would show up in the SEC trace. The high ω section is independent of this, and the plateau modulus is unaffected.

Furthermore, from the plateau modulus, the entanglement molecular weight, M_e, could be calculated as:

$$G_N^0 = \frac{4}{5}\frac{\rho RT}{M_e} \tag{6}$$

where R is the molar gas constant and $\rho = 1.1$ g/cm^3 is the bulk density at $T = 300$ K. It was found that $M_e = 2.16$ kg/mol, in very good agreement with the literature.[15]

In the tube concept for long, entangled polymer chains, the time the chain needs to escape from the tube, the reptation time, is defined as

$$\tau_d = \frac{3N^3 l^2}{\pi^2 W d^2} \tag{7}$$

with N being the number of segments. $l^2 = 33.75$ Å ^{2} is the average monomer length squared[16] and d the tube diameter. The Rouse rate W is related to the friction of a polymer segment in a heat bath ζ_0 as described in the Rouse model for short, unentangled polymer melts:[17,18]

$$Wl^4 = \frac{3k_B T l^2}{\zeta_0} \tag{8}$$

From the loss peak position, ω_{max} of $G''(\omega)$, an effective reptation time τ_d could be extracted as $\tau_d^{exp} = 1/\omega_{max}$. The experimental reptation time τ_d^{exp} is reduced compared to the one proposed by tube theory. This is due to contour length fluctuations of the tube:

$$\tau_d^{exp} = \tau_d^{CLF} = \tau_d\left(1 - \frac{C}{\sqrt{Z}}\right)^2 \tag{9}$$

Here, C is a numerical constant between 1 and 1.47, as estimated in ref 19, and Z is the number of entanglements $Z = N/N_e$, where N_e is the number of monomers (with monomer molecular weight $M_0 = 44$ g/mol) between entanglements, $M_e = N_e M_0$. For high molecular weight polymers, $Z \gg C$ and thus $\tau_d^{exp} \simeq \tau_d$. From this one may independently estimate also the entanglement relaxation time τ_e in terms of the tube model which is defined as the longest relaxation time of a chain with length N_e

$$\tau_e = \frac{\tau_d}{3Z^3} = \frac{N_e^2}{\pi^2 W} \tag{10}$$

Using the WLF shifting parameters $C_1 = 2.306$ and $C_2 = 179.69$ (at the reference temperature, $T_0 = 348$ K) these characteristic relaxation times can be recalculated for any desired temperature: $\tau_e(T) = a_T\tau_e(T_0)$. The times extracted in this way, calculated at $T = 348$ K, for the two high molecular weight samples yield $\tau_e = 23$ ns for the PEO with $M_w = 610$ kg/mol and $\tau_e = 15$ ns for the PEO with $M_w = 932$ kg/mol. In view of the crude approximations here, the agreement is fair enough.

For the low molecular weight sample on the other hand, the accessible temperature range is small. On the low temperature side it is limited by crystallization, for high temperatures the viscosity becomes too low for accurate rheological measurements. Therefore, the only dynamical parameter, which could be reliably measured by rheology in a small T-interval, thereby with constant density, is the zero shear viscosity, η_0. The values extracted from the loss modulus, $\eta_0 = \lim_{\omega\to 0} G''(\omega)/\omega$, are collected in Table 2.

B. Neutron Scattering. The NSE results obtained for the low molecular weight sample are shown in Figure 2.

As mentioned above, for unentangled polymer chains, one expects free Rouse-like behavior. The single chain dynamic structure factor in the Rouse model is given by:

$$S(Q,t) = \frac{1}{N}\sum_{i,j}\exp\left[-Q^2Dt - \frac{1}{6}Q^2|i-j|l^2 - \frac{2Q^2Nl^2}{3\pi^2}\sum_{p=1}\frac{1}{p^2}\cos\left(\frac{p\pi j}{N}\right)\cos\left(\frac{p\pi i}{N}\right)[1-\exp(-tp^2/\tau_R)]\right] \tag{11}$$

Here, i, j are indices for the segments. The first part in the exponential describes the center of mass diffusion with diffusion constant D and the second represents the structure of the chain while the third part is determined by a sum over all internal Rouse modes p of the polymer chain. $\tau_R = N^2/N_e^2\tau_e$ is the longest relaxation time of the chain with N segments.

The solid lines in Figure 2 represent a fit to the NSE data with eq 11. It can be seen that for the short, unentangled chain

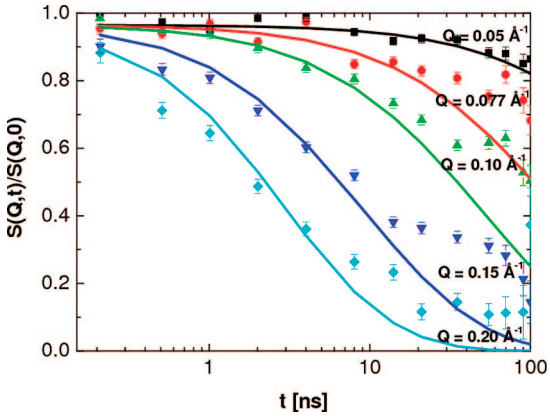

Figure 3. NSE data of a PEO sample with $M_w = 81$ kg/mol at $T = 400$ K. The symbols show the data measured for various Q values. Solid lines represent a fit with the Rouse model simultaneously to all Q values. The data were fitted up to $t = 10$ ns and then extrapolated to observe the expected deviation from the Rouse behavior at longer times.

($M_w \leq M_e$) the Rouse model describes the data very well in the full probed time range. The segmental friction coefficient ζ_0 was fitted simultaneously for all Q values as the only free parameter. The resulting characteristic Rouse rate is equal to $Wl^4 = 21\,750$ Å^4/ns.

For the long polymer chains, the Rouse model starts to fail at $t \simeq 10$ ns (Figure 3).

Obviously, the topological confinements due to the entanglements (the number of entanglements $Z \simeq 38$ per chain for the investigated $M_w = 81$ kg/mol PEO) leads to the much slower reptational motion.[17,20] At longer times $t > 10$ ns one observes well pronounced plateaus, typical for long, entangled chains. This will be discussed below in more detail.

IV. Discussion

A. Segmental Friction. An appropriate way to compare the dynamics of PEO observed for different molecular weights and temperatures, is to focus on the monomeric friction coefficient, ζ_0 which is a central quantity concerning the used techniques. This representation is very convenient for the NSE data where ζ_0 can be directly extracted from the Rouse regime whereas in case of rheology data the zero shear viscosity, η_0, can be used to extract it. For low molecular weight polymers, $M_w < M_e$, the monomeric friction is calculated from

$$\zeta_0 = \frac{36}{N_{Av}} \frac{M_0 \eta_0^{Rouse}}{\rho l^2 N} \tag{12}$$

Here, N_{Av} is the Avogadro number.

For long entangled melts, where the dynamics is governed by tube confinement, the reptational model predicts ideally

$$\eta_0^{reptation} = q\eta_0^{Rouse}\left(\frac{M}{M_e}\right)^2 \tag{13}$$

The prefactor q for pure reptation is usually taken as 15/4 in the literature.[17] However, taking into account constraint release processes this prefactor has to be modified according to refs 15 and 21. Thereby the shift in viscosity due to constraint release as derived in the state of the art theory presented in ref 19 is taken into account. Using the relevant parameters for PEO,[15] q is calculated to be $q = 1.03$. The obtained results for NSE (from direct fitting with the Rouse model) and for the rheology measurements (from eqs 12 and 13), are given in Table 3.

For a precise comparison one has also to take into account the M_w dependence of the glass transition temperature. Since it is known that in the range of low M_w, T_g strongly depends on the molecular weight, the data need to be compared at temperatures which have the same distance to the glass transition temperature.[24,25] As a reference, we have chosen the sample with $M_w = 2.1$ kg/mol which has a $T_g = 199$ K. Since the monomeric friction coefficients were determined as a function of temperature a spline interpolation allows to determine them at any temperature inbetween and the correction for the T_g distance is automatically done. A more subtle way to follow is through the well-known relationship of WLF. Here, only C_1 and C_2 have to be known at the reference temperature T_0 and with the WLF equation, the friction coefficient can be estimated within error bars due to uncertainties in the experimental constants C_1 and C_2 at any temperature. Using the equation

$$a_T = \frac{\zeta_0(T)T_0}{\zeta_0(T_0)T} \tag{14}$$

which is analogous to the WLF equation,[23] we confirm that $\xi_0(T_0)$ from all different measurements at different temperatures is identical to about $1.2 \cdot 10^{-20}$ kg/ns. The correction for the shift in T_g is then easily obtained from $a_{T+\Delta T_g}/a_T$, which, when applied to the NSE results ($M_w = 81$ kg/mol), backscattering (BS) data ($M_w = 24$ kg/mol),[22] and rheology data ($M_w = 0.89$ kg/mol) in Table 3, yields Figure 4. Note, however, that this is only a minor correction.

Table 3. Monomeric Friction Coefficient Obtained from the NSE, Neutron Backscattering (BS, from Ref 22) and Rheology Experiments for the PEO Samples with Different M_w as a Function of Temperature

experimental technique	M_w [kg/mol]	T_g [K]	ζ_0 [10^{-20} kg/ns] (T [K])
rheology	0.89	190	3.885 (308)
			3.389 (313)
			2.680 (318)
			2.187 (323)
NSE	2.1	199	0.225 (413)
BS[a]	24	210	1.327 (350)
			0.669 (375)
			0.435 (400)
NSE	81	210	0.911 (360)
			0.370 (400)
			0.306 (425)
			0.215 (450)
rheology	610	210	0.801 (348)
rheology	932	210	0.444 (378)

[a] From ref 22 the absolute value is consistent with ref 23 and is 2 orders of magnitude lower.

Obviously, taking into account the shift of the glass transition temperature on the probed dynamics, the data are reduced to a single master curve. Only for the high molecular weight samples as measured by rheology with obvious uncertainties we observe deviations. For these materials, the calculated monomeric friction coefficient (eqs 12 and 13) is underestimated. It should be noted that similar discrepancies in the friction coefficient measured by NSE and rheology for the long chains were already found for other polymers e.g. PEP[26] and PI.[21] In case of the long entangled chains, the probed dynamics can not be easily related to the segmental friction as in the case of free Rouse motion. Apparently the more reliable method to extract the friction coefficient would be using its relation to τ_e, i.e. doing a complete fit of G' and G'' by a microscopic theory accounting for the Rouse dynamics, like that presented in ref 19. We have found that using such an evaluation, which also includes contour length fluctuations and constraint release effects, accounts for the observed discrepancies for a PEP sample.[26] For the PEO the situation remains more complicated because due to the crystallization the full dynamical spectrum cannot be accessed. The Rouse regime at high frequencies is far beyond the experimentally accessible range. The estimate for τ_e from the

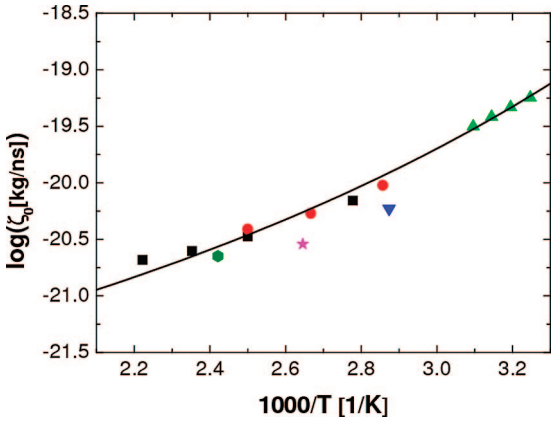

Figure 4. Monomeric friction coefficient obtained experimentally by NSE and rheology for the samples with different molecular weight. The data are compared at a temperature with the same distance to the glass transition temperature (using sample with $M_w = 2.1$ kg/mol as reference). The symbols corresponds to the different molecular weight samples: black squares, $M_w = 81$ kg/mol (NSE); red circles, $M_w = 24$ kg/mol (backscattering);[22] green triangles up, $M_w = 0.89$ kg/mol (rheology); blue triangle down, $M_w = 610$ kg/mol (rheology); pink star, $M_w = 932$ kg/mol (rheology); olive diamond, $M_w = 2.1$ kg/mol (NSE). Line: see text.

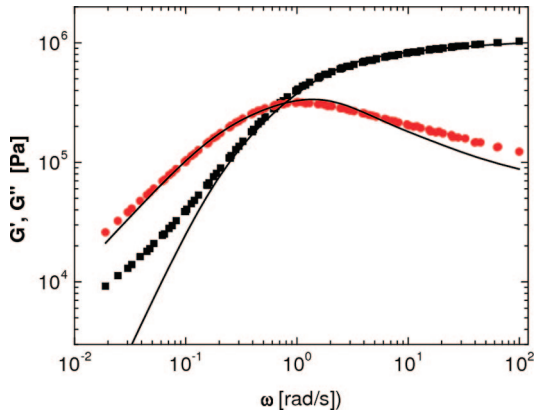

Figure 5. Rheology data for the PEO sample with $M_w = 610$ kg/mol measured at temperature $T = 348$ K. Black squares belong to the storage modulus and red circles to the loss modulus. Lines show the best tentative fitting results obtained with the microscopic model explained in the text.

position of the reptation peak, i.e., from τ_d (eq 10) is highly inaccurate, not only due to the polydispersity and the shape of the peak is strongly deformed. Therefore, the data could not be reliably fitted with a microscopic theory as in ref 19. In this concept the tube model is corrected for time dependent intra and interchain fluctuations, i.e. contour length fluctuations and constraint release events, respectively.[19] The strength of the constraint release contribution is controlled by an empirical parameter c_ν, which varies between 0 (no contribution of constraint release) and 1 (full contribution). Nevertheless, Figure 5 shows the best fit obtained for the sample with $M_w = 610$ kg/mol. The parameter $Z = 282$ was fixed, while τ_e, the plateau modulus and c_ν were fitted independently to $1 \cdot 10^{-7}$ s, 1.2 MPa and 2.38, respectively. The strong deviations at low frequencies of G' and the high frequency wing of G'' point to enhanced polydispersity and lead to unrealistic values for c_ν.

Already a first rough approximation of τ_e calculated from the peak positions of G'', without implementing any theories, gives a factor ~1.5 difference between these two samples, which comes from the uncertainty of M_w, the distribution and polydispersity.

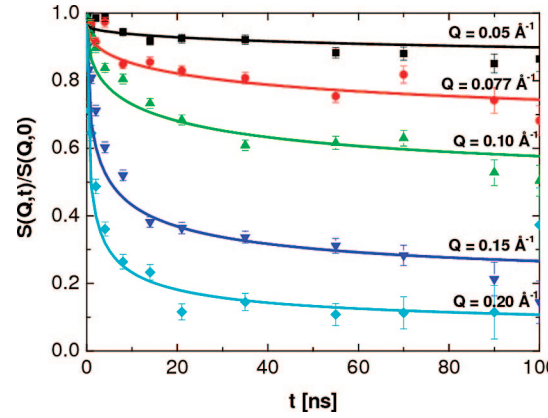

Figure 6. NSE data of a PEO sample with $M_w = 81$ kg/mol at $T = 400$ K. Symbols show the data measured for various Q values. The solid lines represent a fit with the reptation model simultaneously to all Q values. The data were fitted in the time range $t > 10$ ns and then extrapolated to $t = 0$.

Table 4. PEO 81 kg/mol Characteristic Dynamical Parameters

T [K]	Wl^4 [Å^4/ns]	d [Å]	τ_e [ns]
360[a]	5523		
400	15091	52.6	51.2
425	19429	52.6	39.8
450	29280	53.5	28.4

[a] For this temperature the expected crossover time, τ_e, is longer than the maximum measured Fourier time.

Going back to the friction factors (Figure 4), the observed temperature dependence of the friction follows a Vogel-Tammann-Fulcher (VTF) law:

$$\zeta = \zeta_0^\infty \exp(B/(T - T_\infty)) \tag{15}$$

where B is the VTF parameter and T_∞ is the VTF temperature. T_∞ was taken from ref 27. However, since the value there was given for high molecular weight PEO it was shifted by the difference in the glass transition temperatures ($\Delta T_g = 11$ K) yielding $T_\infty = 155$ K for our low molecular weight ($M_w = 2.1$ kg/mol) PEO. The obtained VTF fitting parameters are: $\zeta_0^\infty = 4.65 \times 10^{-23}$ kg/ns, $B = 1090$ K.

The representation used above in Figure 4, where the logarithm of monomeric friction coefficient is plotted versus $1/T$, is the so-called Angell fragility plot.[28] For the glass forming polymer systems, displaying a VTF temperature dependence, the fragility m is conveniently defined in terms of effective activation enthalpy at $T = T_g$:

$$m = \left.\frac{\mathrm{d}(\log \zeta_0)}{\mathrm{d}(T_g/T)}\right|_{T=T_g} = \frac{BT_g}{(T_g - T_\infty)^2} \tag{16}$$

The value calculated for PEO, in reference to the sample with $M_w = 2.1$ kg/mol is $m = 108$, i.e. is in good agreement with literature values for PEO.[29]

B. Confined dynamics. Following equation 6 the tube diameter d can be calculated as[30–32]

$$d^2 = \frac{4}{5}\frac{R_E^2}{M}\frac{\rho RT}{G_n^0} = R_E^2\frac{M_e}{M} \tag{17}$$

where $R_E^2 = l^2 M/M_0$ is the end-to-end distance of the chain and M is the molecular weight of the probed polymer chain. The tube diameter estimated in this way from rheology experiment is $d = 40.7$ Å.

In the NSE data for the long chain melt, we evidently observe confined motion, and the single chain dynamic structure factor shows a plateau characteristic for reptation-like dynamics; see

Figure 6. In the tube model, the single chain dynamic structure factor is determined by two processes: local reptation describes a Rouse-like motion of a confined chain; i.e., in contrast to a free chain the movement is reduced to one dimension along the tube profile. The second term accounts for the center of mass diffusion of the chain out of the tube, therefore called the creep or escape term.

$$\frac{S(Q,t)}{S(Q)} = (1 - F(Q))S_{\text{loc rep}}(Q,t) + F(Q)S_{\text{esc}}(Q,t) \quad (18)$$

Here, $F(Q)$ is the (cross-sectional) form-factor of the tube:

$$F(Q) = \exp[-(Qd/6)^2] \quad (19)$$

The relaxation time of the escape term is the reptation time as defined in eq 7. Since this time is proportional to N^3, for the here discussed chain with $M_w = 81$ kg/mol, $\tau_d \approx 1$ ms is far beyond the time window of the NSE experiment. Therefore $S_{esc}(Q, t) = 1$. The contribution of the local reptation process is given by:

$$S_{\text{loc rep}}(Q,t) = \exp\left(\frac{t}{\tau_0}\right)\text{erfc}\left(\sqrt{t/\tau_0}\right) \quad (20)$$

The time scale in eq 20 is given by $\tau_0 = 36/(Wl^4Q^4)$ for Rouse type segment diffusion along the tube.

Note that the reptational dynamic structure factor as defined in eq 18 does not account for the short time Rouse dynamics. Therefore, the data were fitted with the tube model only at longer times, in the plateau region for $t > 10$ ns; see Figure 6. In the fitting procedure, the characteristic Rouse rate was fixed to the value found earlier from the Rouse fit at short times, for the same sample. Thus, the fit simultaneously to all Q values was performed with only one free parameter, namely the tube diameter. The results presented in Figure 6 show that the experimental data follow nicely the behavior predicted by the tube model.

The results obtained for the tube diameter and consequently the expected theoretically crossover time from Rouse to reptation motion at τ_e (see eq 10) obtained at different temperatures are given in Table 4.

The results show, that in the temperature range of observation 400 K $\leq T \leq$ 450 K the tube diameter is nearly constant for the investigated PEO system. Moreover, the tube diameter found by rheology ($d = 40.7$ Å) is by a factor ~1.3 smaller than that obtained from the NSE experiment ($d \simeq 53$ Å).

An interpretation of these results requires detailed understanding of the entanglement phenomenon on the microscopic and molecular level. The viscoelastic properties of high molecular weight polymer melts are, based on the analogy to a rubber elasticity, ascribed to a formation of a temporary cross-linked network. In the tube theory the mesh size of network is identified with the lateral confinement in terms of the tube diameter. Different ideas like the scaling models were proposed in order to describe formation of entanglements and its main features. Examples are the general scaling ansatz proposed by Graessley and Edwards, where it is assumed that the entanglements are determined by the chain contour length density,[33] the binary contact model proposed by de Gennes[34] and Edwards[35] relating entanglements to the interchain contacts or the packing models addressed by Ronca,[36] Lin[37] and Kavassalis and Noolandi.[38] An other model considers entanglements to be purely geometrical effect - a topological approach. There the constraints are calculated in terms of mathematical models, like proposed by Edwards[39] and Edwards and Iwata.[40]

The temperature dependence of d as defined in ref 17 is obviously given by the proportionality of d^2 to T and $\rho(T)$. These dependencies roughly cancel as shown by the temperature dependent vertical shift factors in rheology which are approximately 1. Therefore, independent of the assumed approach, the expected temperature dependence of the characteristic length scale of the confinement is mainly determined by the characteristic ratio C_∞. However, it was shown that the C_∞ for PEO is hardly changing with temperature (in the temperature range 360 K $\lesssim T \lesssim\leq$ 450 K, $C_\infty \simeq 5$).[16] Thus, we also do not expect any temperature dependence for the tube diameter.

Concerning the differences in the results obtained from rheology and NSE (difference by a factor of ~1.3), similar discrepancies were found already earlier for PE and PEP.[41] Their origin is still unclear but may be related to different length scales probed in rheology and NSE. In particular it is up to now not clear whether there exist two confinement length scales one parallel and one perpendicular to the chain contour. In that case it may be possible that different techniques measure different averages of these values.

V. Conclusions

This study on the dynamics of a PEO polymer melt over a wide range of molecular weights and temperatures combines different experimental techniques, rheology and NSE to observe dynamics on macroscopic as well as on molecular length scales. The viscoelastic properties and the single chain dynamic structure factor were investigated dependent on temperature and molecular weight. The obtained results shows that the monomeric friction coefficient at temperatures at constant distance from the glass transition temperature can be well described by the VTF temperature dependence, relative to the predefined T_∞. Furthermore, we also observed that the monomeric friction coefficient, which was extracted from the nonentangled viscoelastic relaxation modulus based on the Rouse model is in good accordance with the data obtained directly from NSE measurements. On the other hand, the tube diameter was found to be independent of the temperature in the measured temperature range, which may be expected for a constant C_∞. The discrepancies for the tube diameter, however, between the NSE and rheology results observed for the high molecular weight samples remain unsolved. The discrepancies in the monomeric friction coefficient on the other hand may be related to the way how the friction is extracted from rheology data and to the inferior quality of the high molecular weight samples.

Acknowledgment. This work utilized facilities supported in part by the National Science Foundation under Agreement No. DMR-0454672.

References and Notes

(1) Addai-Mensah, J.; Yeap, K. Y.; McFarlane, A. J. *Powder Technol.* **2007**, *179* (1−2), 79–83.
(2) Ramachandran, R. *Plastics Eng.* **1996**, *52* (4), 31.
(3) Altaf, S. A.; Hoag, S. W.; Ayres, J. W. *Drug Dev. Ind. Pharm.* **1998**, *24*, 737–746.
(4) Gutzler, R.; Smulders, M.; Lange, R. F. *Macromol. Symp.* **2005**, *225*, 81–93.
(5) Wilson, J. S.; Frampton, M. J.; Michels, J. J.; Sardone, L.; Marletta, G.; Friend, R. H.; Samori, P.; Anderson, H. L.; Cacialli, F. *Adv. Mater.* **2005**, *17*, 2659.
(6) Maitra, A.; Heuer, A. *Phys. Rev. Lett.* **2007**, *98*, 227802.
(7) Niedzwiedz, K.; Wischnewski, A.; Monkenbusch, M.; Richter, D.; Genix, A.-C.; Arbe, A.; Colmenero, J.; Strauch, M.; Straube, E. *Phys. Rev. Lett.* **2007**, *98* (16), 168301.
(8) Ratna, D.; Divekar, S.; Patchaiappan, S.; Samui, A. B.; Chakraborty, B. C. *Polym. Int.* **2007**, *56*, 900–904.
(9) The identification of any commercial product or trade name does not imply endorsement or recommendation by the National Institute of Standards and Technology.
(10) Van Krevelen, D. W. *Properties of polymers*; Elsevier Scientific Publishing Company: Amsterdam, 1976.
(11) Silvestre, C.; Cimmino, S.; Martuscelli, E.; Karasz, F. E.; MacKnight, W. J. *Polymer* **1987**, *28*, 1190–1199.

(12) Mezei, F. *Neutron spin echo spectroscopy*; Lecture Notes in Physics 128; Springer Verlag: Berlin, Heidelberg, Germany, and New York, 1979.
(13) Richter, D.; Monkenbusch, M.; Arbe, A.; Colmenero, J. *Adv. Polym. Sci.* **2005**, *174*, 1.
(14) Jackson, J. K.; Winter, H. H. *Rheological Acta* **1996**, *35*, 645–655.
(15) Fetters, L. J.; Lohse, D. J.; Milner, S. T.; Graessley, W. W. *Macromolecules* **1999**, *32*, 6847.
(16) Smith, G. D.; Yoon, D. Y.; Jaffe, R. L.; Colby, R. H.; Krishnamoorti, R.; Fetters, L. J. *Macromolecules* **1996**, *29*, 3462–3469.
(17) Doi, M.; Edwards, S. F. *The Theory of Polymer Dynamics*; Oxford University Press: Oxford, U.K., 1986.
(18) Rouse, P. E. *J. Chem. Phys.* **1953**, *21*, 1272–1280.
(19) Likhtman, A. E.; McLeish, T. C. B. *Macromolecules* **2002**, *35*, 6332–6343.
(20) de Gennes, P.-G. *J. Phys. (Paris)* **1981**, *42*, 735–740.
(21) Abdel-Goad, M.; Pyckhout-Hintzen, W.; Kahle, S.; Allgaier, J.; Richter, D.; Fetters, L. J. *Macromolecules* **2004**, *37*, 8135–8144.
(22) Genix, A.-C.; Arbe, A.; Alvarez, F.; Colmenero, J.; Willner, L.; Richter, D. *Physical Review E* **2005**, *72* (3), 31808–31820.
(23) Ferry, J. D. *Viscoelastic Properties of Polymers*; John Wiley & Sons: New York, 1980.
(24) Pearson, D. S.; Fetters, L. J.; Graessley, W. W.; Strate, G. V.; Vonmeerwall, E. *Macromolecules* **1994**, *27*, 711–719.
(25) Pearson, D. S.; Fetters, L. J.; Younghouse, L. B.; Mays, J. W. *Macromolecules* **1988**, *21*, 478–484.
(26) Niedzwiedz, K.;Wischnewski, A.;Pyckhout-Hintzen, W.;Willner, L.;Richter, D. To be published.
(27) Lutz, T. R.; Yiyong, H.; Ediger, M. D.; Haihui, C.; Guoxing, L.; Jones, A. A. *Macromolecules* **2003**, *36*, 1724–1730.
(28) Angell, C. A.; Sichina, W. *Ann. N.Y. Acad. Sci.* **1976**, *279* (Oct 15), 53–67.
(29) Carini, G.; D'Angelo, G.; Tripodo, G.; Bartolotta, A.; Di Marco, G. *Phys. Rev. B* **1996**, *54*, 15056.
(30) Doi, M.; Edwards, S. F. *J. Chem. Soc., Faraday Trans. 2* **1978**, *74*, 1789–1801.
(31) Doi, M.; Edwards, S. F. *J. Chem. Soc., Faraday Trans. 2* **1978**, *74*, 1802–1817.
(32) Doi, M.; Edwards, S. F. *J. Chem. Soc., Faraday Trans. 2* **1979**, *75*, 38–54.
(33) Graessley, W. W.; Edwards, S. F. *Polymer* **1981**, *22*, 1329–1334.
(34) deGennes, P.-G. *J. Phys. Lett.* **1974**, *35*, L217.
(35) Edwards, S. F. *Proc. Phys. Soc. London* **1967**, *92* (575P), 9.
(36) Ronca, G. J. *J. Chem. Phys.* **1983**, *79*, 1031–1043.
(37) Lin, Y. H. *Macromolecules* **1987**, *20*, 3080–3083.
(38) Kavassalis, T. A.; Noolandi, J. *Macromolecules* **1988**, *21*, 2869–2879.
(39) Edwards, S. F. *Proc. R. Soc. London, Ser. A* **1988**, *419* (1857), 221–234.
(40) Iwata, K.; Edwards, S. F. *J. Chem. Phys.* **1989**, *90*, 4567–4581.
(41) Wischnewski, A.; Monkenbusch, M.; Willner, L.; Richter, D.; Kali, G. *Phys. Rev. Lett.* **2003**, *90*, 058302.

MA800446N